AN EXPERIMENTAL STUDY ON THE STATIC AND DYNAMIC

CHARACTERISTICS OF PUMP ANNULAR SEALS

T. Iwatsubo, B.C. Sheng, and T. Matsumoto
Faculty of Engineering
Kobe University
Rokko, Nada, Kobe, Japan

E-4227-13

A new test apparatus is constructed and is applied to investigate static and dynamic characteristics of annular seals for turbopumps. The fluid forces acting on the seals are measured for various parameters such as the preswirl velocity, the pressure difference between the inlet and outlet of the seal, the whirling amplitude, and the ratio of whirling speed to spinning speed of the rotor. Influence of these parameters on the static and dynamic characteristics is investigated from the experimental results. As a result, preswirl affects the dynamic characteristics strongly. Especially, the preswirl opposing the rotating direction has a stabilizing role on the rotor system.

1. Introduction

A turbomachine such as a pump tends to be operated at high speed and high pressure because of severe performance requirements. But with increasing speed and pressure, the fluid force causes an instability of the rotating machine because of the noncontacting seal, such as the balance piston and wear ring. So, it is necessary to make the dynamic behavior clear and to supply accurate data in order to predict and prevent the unstable vibration, and still more necessary to design a stable rotating machine.

Many theoretical and experimental analyses on the characteristics of noncontacting seals are reported. As an experimental research on annular seals, Childs et al. (Refs. 2,3) investigated fluid forces acting on the seals and their characteristics with a test apparatus which has an eccentric rotor. Nordmann (Ref. 4) used an impulse force type test apparatus to carry out an experiment on the characteristics of annular seals. Kaneko et al. (Ref. 7), Kanki et al. (Ref. 8), and Hori et al. (Ref. 9) also reported their test results on the seals. All these results are important for the research on annular seals. However in these experimental apparatus, the casing inertia force of the test rig is larger than the flow-induced force due to the seal, so the signal/noise ratio is not good. Childs et al. investigated the characteristics under the condition of rotor whirling motion, but limited by the test apparatus, he only investigated the characteristics in the synchronous motion of the rotor. Recently, Kanemori and Iwatsubo (Ref. 10) used a test apparatus in which the rotor gives spinning and whirling motion independently to test a long annular seal of a submerged pump for various whirling speeds. But, they did not test for the preswirl velocity, which strongly affects the stability of a rotor system, because their interest is limited to the dynamic

characteristics of the submerged pump. The dynamic characteristics of annular seals have not been investigated yet in various operating conditions.

This paper shows the experimental results obtained by an experimental apparatus which is newly designed to obtain a high S/N ratio. In the test the fluid force acting on the seals is measured and the stiffness, damping, and inertia coefficients are obtained. Influence of the parameters such as the whirling amplitude pressure difference between the inlet and outlet of the seal, preswirl, rotating and whirling speeds, and their directions is investigated.

2. Nomenclature

Fx,Fy   : Fluid forces in x and y directions
Fr,Ft   : Fluid forces in r and t directions
Kxx,Kyy,Kxy,Kyx   : Stiffness coefficients
Cxx,Cyy,Cxy,Cyx   : Damping coefficients
Mxx,Myy,Mxy,Myx   : Inertia coefficients
x,y,z   : Fixed coordinates
r,t   : Radial and tangential coordinates
$p(\phi,z)$: Pressure distribution
$P(\phi)$: Average pressure in axial direction
Pin   : Inlet pressure to the seal
Pex   : Outlet pressure from the seal
ΔP : Pressure difference between inlet and outlet of the seal
ω : Spinning angular velocity of the rotor
Ω : Whirling angular velocity of the rotor
e   : Whirling eccentricity of the rotor
ϕ : Phase difference between principle force and displacement
R,D   : Rotor radius and diameter, respectively
L   : Seal length
C   : Seal clearance
Vt   : Preswirl velocity
Vts   : Preswirl velocity without a rotating motion
Va   : Fluid average velocity in axial direction

3. Test apparatus and measuring instruments

3.1 Test apparatus

Figs. 1 and 2 show the assembly of the test apparatus and the layout of the test facility, respectively. In Fig. 1, a working fluid, that is, water, is injected through three pairs of swirl passages to accomplish the different inlet swirl velocities shown in cross section B. The water passes through the clearances of the seal and flows to outlets in both sides of the housing. Cool water is continuously applied to the tank in order to maintain constant water temperature.

The inlet part consists of six tubes connected with swirl passages for injecting the water, and swirl speed is adjusted by the six valves in order to obtain the arbitrary swirl velocity in the range of 0 - 6.5 m/s.

The seal assembly consists of a seal stator and a seal rotor. The seal rotor, of which the diameter is 70 mm, is connected to the motor by a flexible coupling. The motor is controlled in the speed range 0 - 3500 r.p.m. by an electric inverter, which also selects the rotational direction. The four types of parallel annular seals shown in Table 1 were prepared for the test. The seal stator has holes to measure the dynamic pressure in the seal, as shown in cross section C. Both long
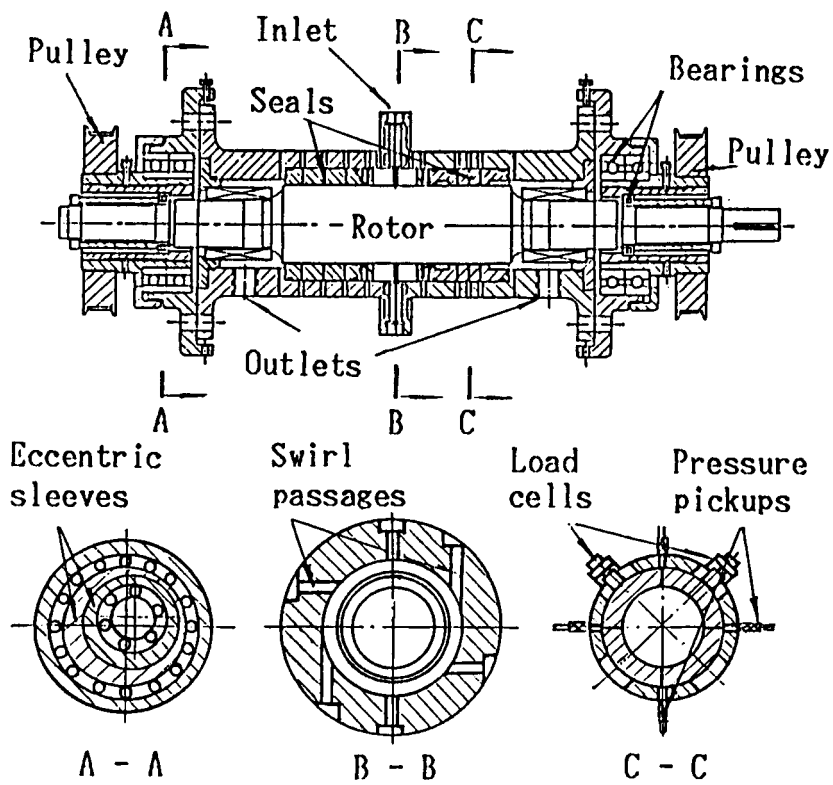
Fig.1 Test apparatus assembly
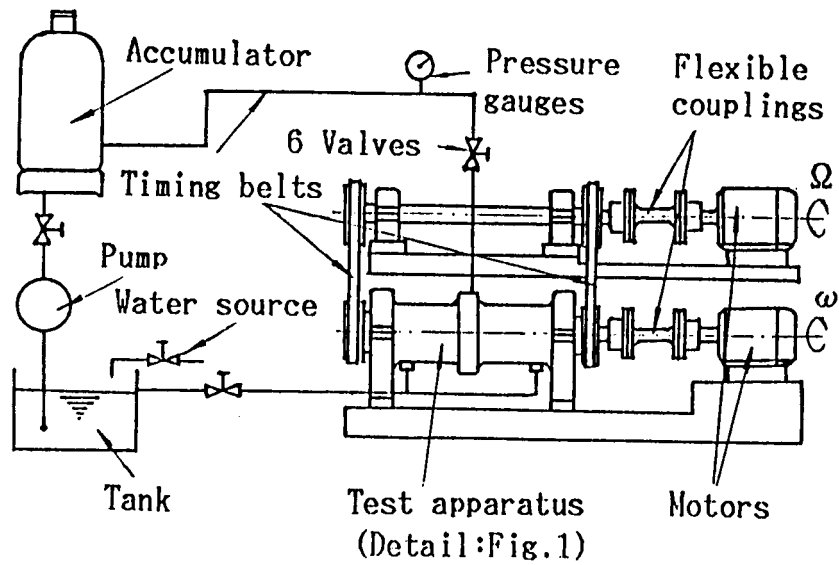
Fig.2 Test facility layout

Table 1 Specifications of seals

	Length (mm)	Diameter (mm)	L/D	Clearance (mm)
Seal 1	70	70	1.0	0.175
Seal 2	35	70	0.5	0.175
Seal 3	70	70	1.0	0.5
Seal 4	35	70	0.5	0.5

and short seals have three holes in the axial direction and four holes in the x and y directions. The dynamic pressure is measured by the strain gauge type pressure gauge shown in cross section C. The fluid dynamic force acting on the stator is also directly measured by the load cells shown in cross section C for comparison with the data of the pressure transducers.

The bearing assembly has two ball bearings to make spinning and whirling motions. To make a whirling motion, an inside sleeve and an outside sleeve, which have a 0.05 mm eccentricity to each other, are attached between the two bearings as shown in cross section A of Fig. 1. The two eccentric sleeves can be rotated, relatively. So an arbitrary eccentricity can be adjusted in the range of 0 - 0.1 mm. The sleeves of both sides are driven by a motor through the timing belts. The motor can also be controlled by an electric inverter in the rotating speed range of 0 - 3500 r.p.m., and rotational direction can be selected by an inverter.

3.2 Measuring instruments

The measuring procedure illustrated in Fig. 3 consists of four kinds of physical variables: that is, rotating and whirling speed, dynamic pressure in the seal, seal forces, and displacement of the rotor. Signals from measuring instruments are recorded by a data recorder and analyzed by a computer.

The rotating and whirling speed are measured by eddycurrent type pulse sensors and digital counters.
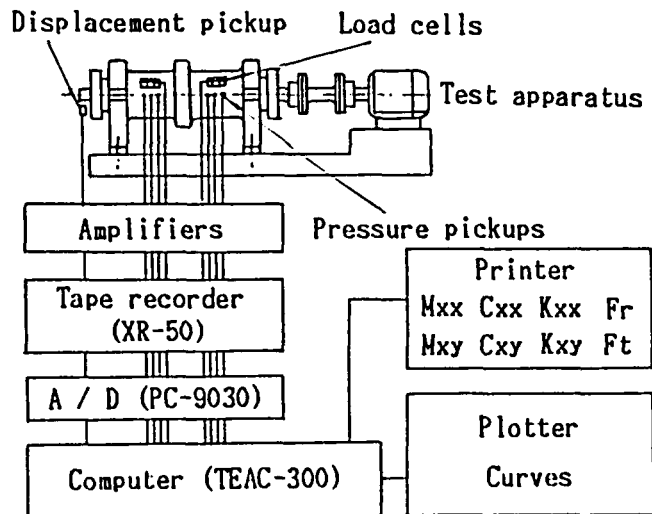
Fig.3 Measurement procedure

A pressure transducer of the semiconductor strain gauge type is used to measure the dynamic pressure through the syringe needle. The pressure in the seal is measured at the three points in the seal shown in Fig. 4. The seal stator is mounted on the housing by O-rings as shown in Fig. 4.

Dynamic fluid force can be directly measured by a load cell as shown in Fig. 5. The force measured by the load cell is calibrated to revise the influence of the O-rings and the inertia of the seal.

An eddycurrent type displacement sensor is used to measure the displacement, and this displacement is used as a reference signal to obtain the phase difference between the displacement and the flow induced force.

The test data are recorded by a data recorder and sent to the computer through an A/D converter. In the computer the pressure values are integrated in the circumferential direction to obtain the fluid force; then the characteristic coefficients are calculated.

A special pitot tube set is used to measure the preswirl velocity in the seal inlet, as shown in Fig. 6. The static and total pressures are measured by the pressure transducers instead of the usual U-tube.

Axial flow velocity in the seal and leakage are determined from the outlet flow velocity directly measured by a pitot tube.

3.3 Calibration

As a preliminary test, the static and dynamic characteristics of measuring instruments (i.e., the pressure transducer, the load cell, and the pitot tube) were calibrated.

Because the pressure measuring set is constructed by a pressure transducer and a syringe needle, a phase difference between real pressure and measured pressure was investigated. Then, it was found that the pressure measuring set has a phase lag relative to the real pressure and that the phase lag increases with the frequency.
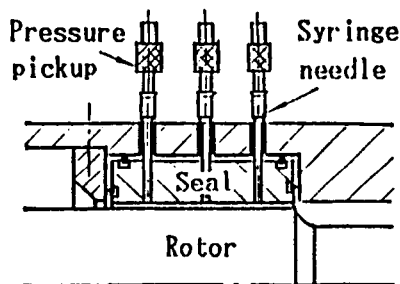
Fig.4 Detail of pressure measurement
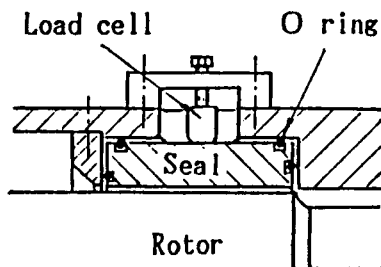
Fig.5 Detail of force measurement

233
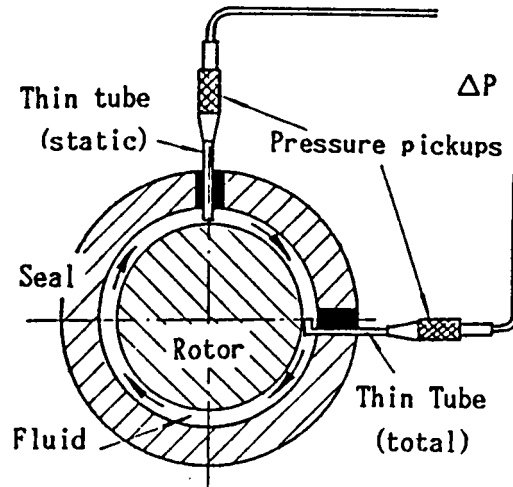
Fig.6 Detail of swirl velocity measurement

Dynamic calibration of the load cell was done in various working conditions. A periodic force was excited on the seal by a shaker, and the force was simultaneously measured by strain gauges attached to the shaking rod and by the load cell fixed on the other side. These data were used to calibrate the measured data in the real test.

A pitot tube set was used to measure the inlet preswirl velocity. Its pitot tube coefficient for calibration was determined by means of a standard pitot tube.

4. Discussions on the accuracy measured by the test apparatus

4.1 Comparison with the data by two measuring methods

Fig. 7 illustrates the fluid forces measured by the load cell unit and the pressure transducer unit. These results show a reasonable agreement because the relative error between the two results is within 5.5 percent.

4.2 Comparison with other researcher's results

A comparison of the authors' experimental results with Childs' (Ref. 2) results is shown in Fig. 8. These results cannot be compared quantitatively, because the working fluids and test conditions are different. However, these results have the same tendencies. Fig. 9 gives the test results of Kanemori et al. (Ref. 10). These results also demonstrate good agreement with the authors' results of Fig. 10.

5. Calculation of fluid force and characteristic coefficients

It is assumed that the motion equation of the rotor system is represented as follows

$$[M]\{\ddot{X}\}+[C]\{\dot{X}\}+[K]\{X\}=\{f(t)\}-\{F\}$$

234
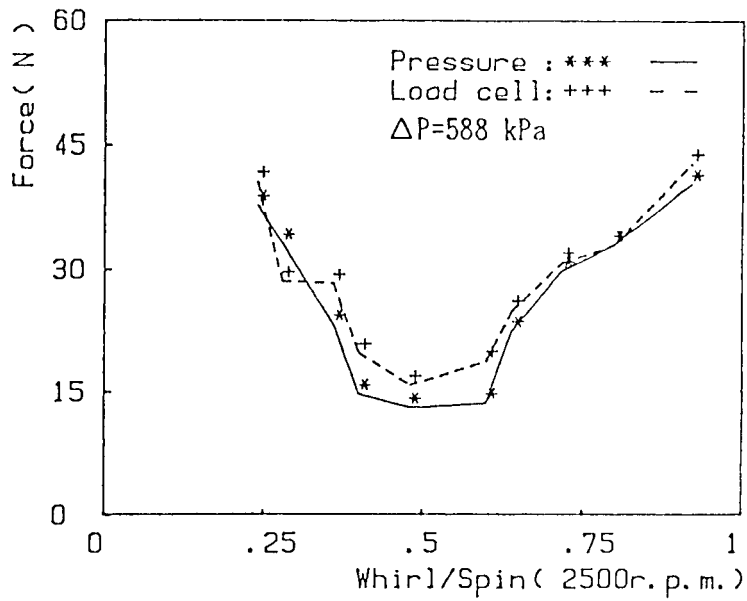
(a) Force
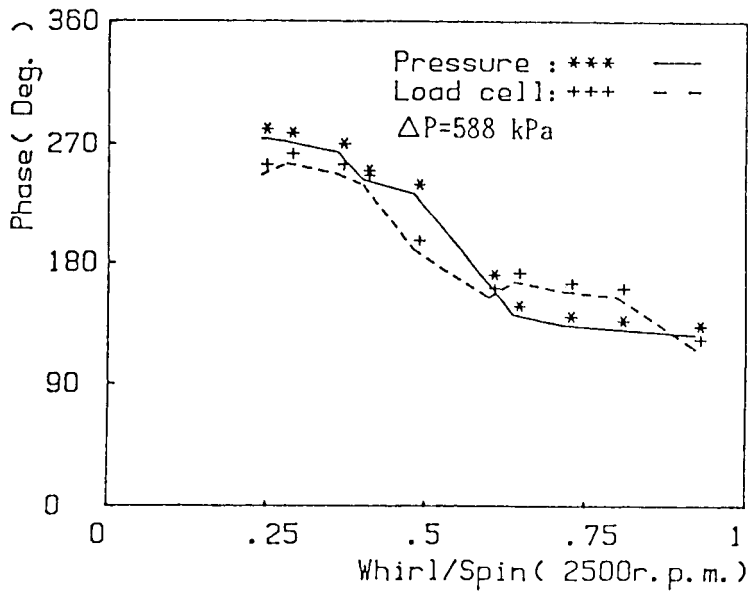
(b) Phase

Fig.7 Results measured by two measuring methods

235
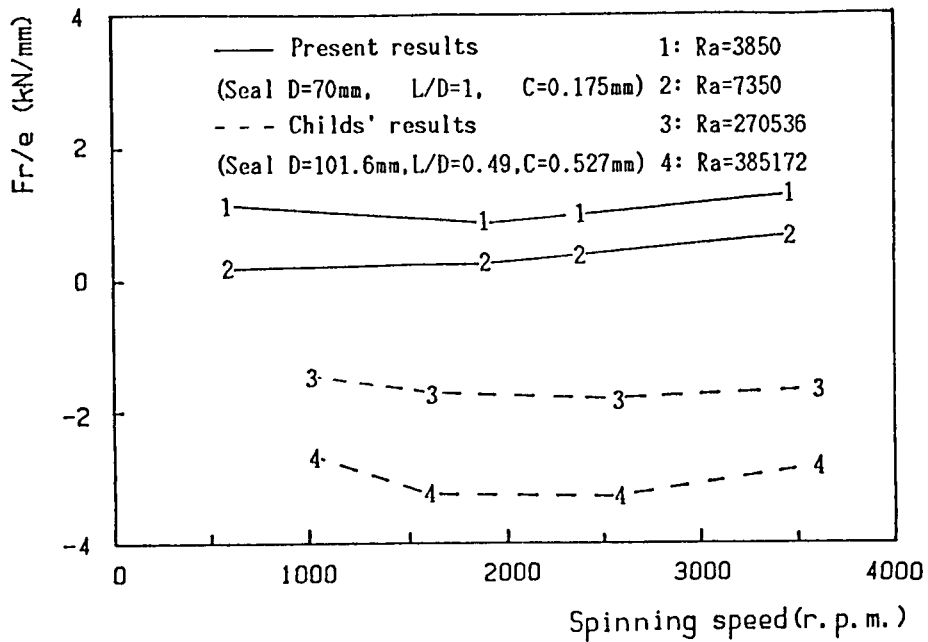
(a) Radial coefficient Fr/e
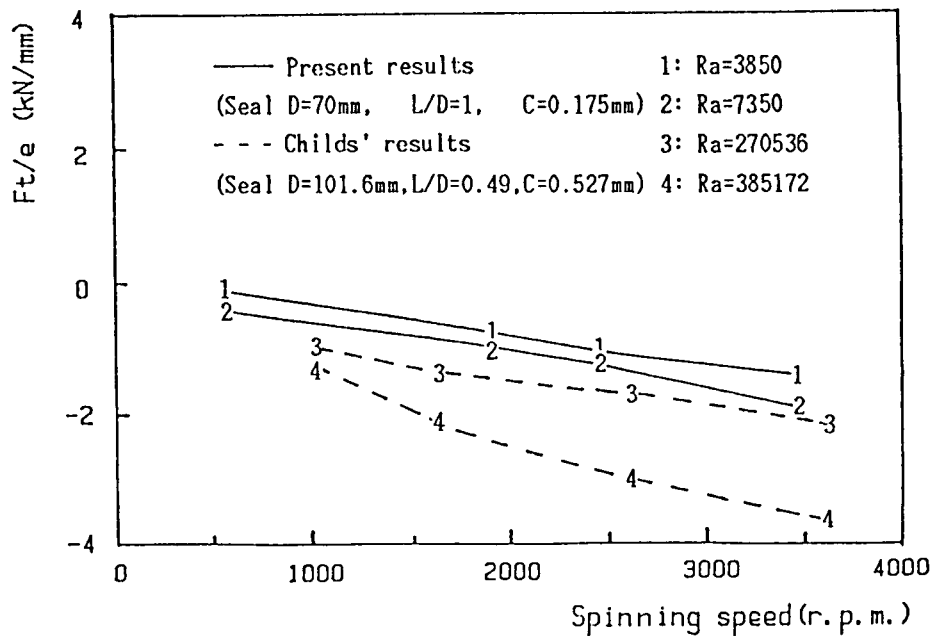
(b) Tangential coefficient Ft/e

Fig.8 Comparison of experimental results and Childs' results

236
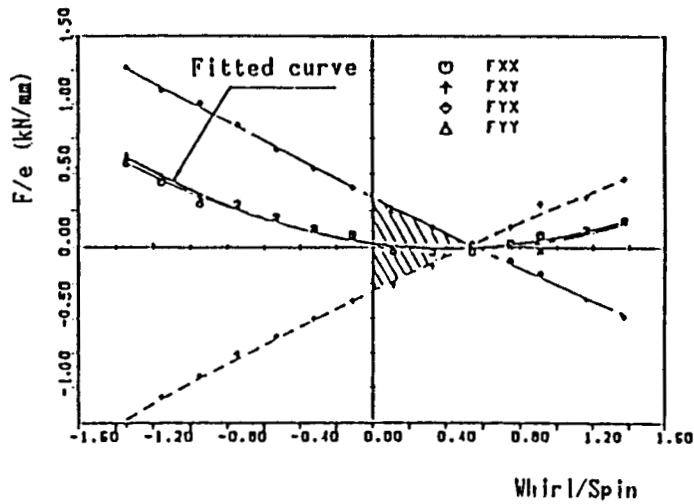
Fig.9 Kanemori's results
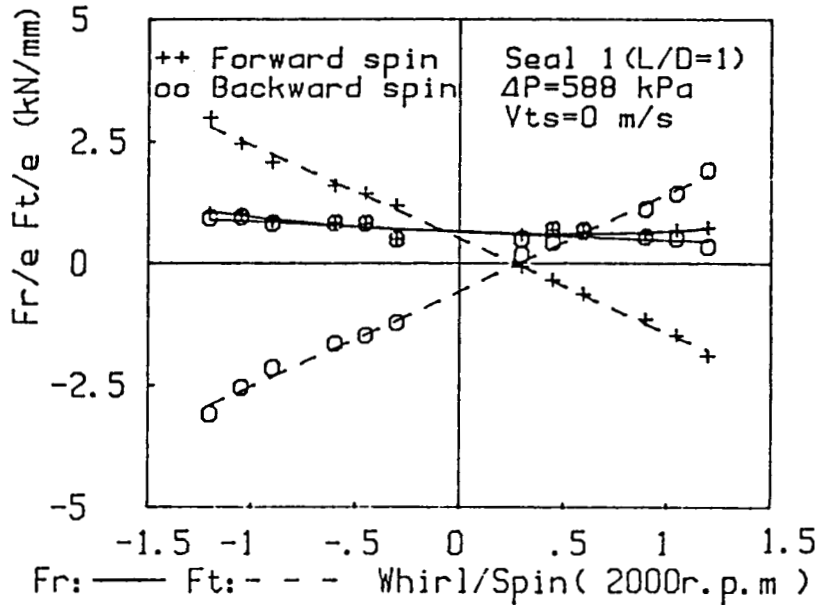
Fig.10 Results for forward and backward spinning speeds

where [M],[C],[K] are the mass, the damping, and the stiffness matrix and {f(t)} is
the force vector. {F}={Fx Fy}^{t} is the fluid reaction force acting on a rotor and
is represented as a linear function of rotor displacement, velocity, and
acceleration, as follows.

$$- \begin{bmatrix} Fx \\ Fy \end{bmatrix} = \begin{bmatrix} Mxx & Mxy \\ Myx & Myy \end{bmatrix} \begin{bmatrix} \ddot{x} \\ \ddot{y} \end{bmatrix} + \begin{bmatrix} Cxx & Cxy \\ Cyx & Cyy \end{bmatrix} \begin{bmatrix} \dot{x} \\ \dot{y} \end{bmatrix} + \begin{bmatrix} Kxx & Kxy \\ Kyx & Kyy \end{bmatrix} \begin{bmatrix} x \\ y \end{bmatrix} \qquad \cdots(1)$$

For a small whirling motion about a center position, the relation of the
coefficients may be expressed by

$$Mxx = Myy, \quad Myx = Mxy = 0, \quad Cxx = Cyy,$$
$$Cyx = -Cxy, \quad Kxx = Kyy, \quad Kyx = -Kxy \qquad \cdots(2)$$

237

where the cross-coupled inertia coefficient is neglected because it is negligibly small.

A rotating coordinate system rotating with the rotor is adopted to analyze the fluid forces easily. The relation between a fixed coordinate system and a rotating coordinate system is illustrated in Fig. 11, where Fx and Fy are represented by the radial force Fr and the tangential force Ft.
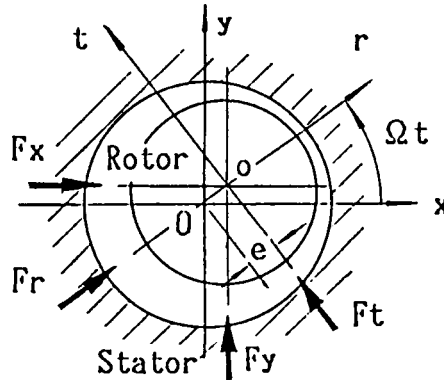
Fig.11 Model of annular seal

In the test, whirling motion is given by

$$
\begin{aligned}
x &= e \cdot \cos\Omega t, & y &= e \cdot \sin\Omega t \\
\dot{x} &= -e \cdot \Omega \cdot \sin\Omega t, & \dot{y} &= e \cdot \Omega \cdot \cos\Omega t \\
\ddot{x} &= -e \cdot \Omega^2 \cdot \cos\Omega t, & \ddot{y} &= -e \cdot \Omega^2 \cdot \sin\Omega t
\end{aligned}
\qquad \cdots (3)
$$

Substituting Eq. (3) and Eq. (2) into Eq. (1), the following expressions are obtained

$$
\begin{aligned}
Fr &= e \ (-Kxx - \Omega Cxy + \Omega^2 Mxx) \\
Ft &= e \ (\ Kxy - \Omega Cxx)
\end{aligned}
\qquad \cdots (4)
$$

or

$$
\begin{aligned}
-Fr/e &= Kxx + \Omega Cxy - \Omega^2 Mxx \\
-Ft/e &= -Kxy + \Omega Cxx
\end{aligned}
\qquad \cdots (5)
$$

where $-Fr/e$ and $-Ft/e$ are called the restitution force coefficient and the tangential force coefficient, respectively.

The displacement of the rotor, the pressure, and the force can be directly measured by the displacement sensor, the pressure transducer, and the load cell, respectively. So the dynamic coefficients are determined from these data.

The fluid forces are obtained by integrating the pressure distribution along the axial and circumferential directions of the seal: that is,

$$Fr = \int_0^L \int_0^{2\pi} p(\phi, z) \cdot \cos\phi \cdot R \cdot d\phi \cdot dz$$

$$= R \cdot L \cdot \int_0^{2\pi} P(\phi) \cdot \cos\phi \cdot d\phi$$

$$= (L \cdot D \cdot \pi / N) \sum_{j=1}^{N} P(\phi j) \cdot \cos\phi j$$

$$\cdots (6)$$

$$Ft = \int_0^L \int_0^{2\pi} p(\phi, z) \cdot \sin\phi \cdot R \cdot d\phi \cdot dz$$

$$= R \cdot L \cdot \int_0^{2\pi} P(\phi) \cdot \sin\phi \cdot d\phi$$

$$= (L \cdot D \cdot \pi / N) \sum_{j=1}^{N} P(\phi j) \cdot \sin\phi j$$

where N is the time series total number of pressures within one period. $P(\phi)$ is average pressure in the axial direction,

$$P(\phi) = (1/L) \int_0^L p(\phi, z) \cdot dz$$

$$= (1/L) \sum_{i=1}^{3} Pi \cdot Li \qquad \cdots (7)$$

where Pi is the pressure measured at different points, and Li is the length between these points.

To determine the coefficients Mxx, Cxx, Cxy, Kxx, and Kxy of Eq. (5), Fr/e and Ft/e at 12 different forward and backward whirling speeds are measured for a given spinning speed, and Ft/e is approximated by a linear function, and Fr/e by a quadratic function of Ω. From Eq. (5), the inertia coefficient, damping coefficients, and stiffness coefficients are represented by the curvature, the slopes, and the crosses, respectively. The experimental conditions are shown in Table 2.

Table 2 Experimental Conditions

Pressure difference Δ P (kPa)	196, 294, 490, 588, 882
Whirling amplitude e (μ m)	20, 30, 40, 50, 60
Spinning speed ω (r.p.m)	500 ~ 3500
Whirling speed Ω (r.p.m)	± 600 ~ ± 2400
Preswirl velocity Vt (m/s)	0 ~ ±13

6. Experimental results and discussion

Since the fluid forces measured by the pressure transducer and load cell are about the same, the fluid force measured by the pressure transducer is used as the experimental results in this discussion.

239

6.1 Pressure distribution and leakage (static results)

The static pressure distributions in the axial direction of seal 1 and 2 are shown in Fig. 12, and the dynamic pressure distributions of seal 1 are shown in Fig. 13 for various inlet pressures. It is known from Fig. 13 that the dynamic pressure distribution is more sensitive to the inlet pressure.

The leakages of seal 1 to 4 are shown in Fig. 14. They increase as the pressure difference and the seal clearance increase but reduce slightly with increasing spinning speeds. Also they are insensitive to the preswirls, whirling amplitude, and whirling speeds of the rotor.
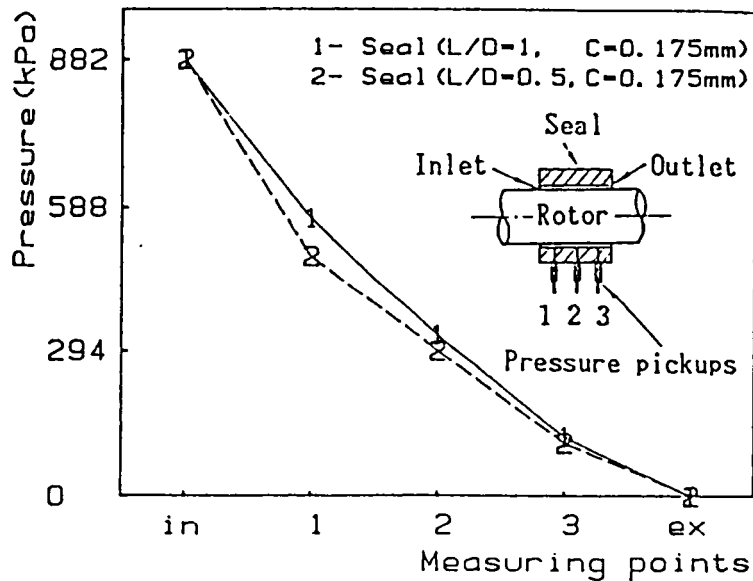
Fig.12 Static pressure falls
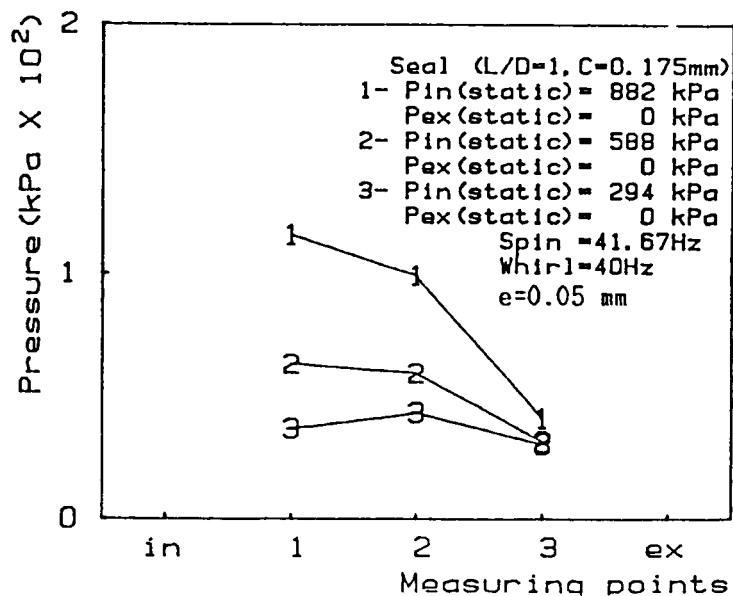
Fig.13 Dynamic pressure falls
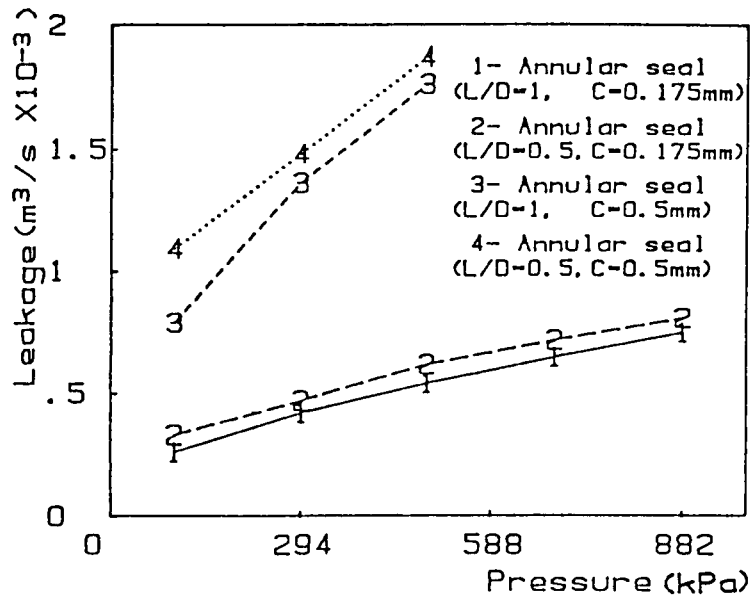
Fig.14 Leakages
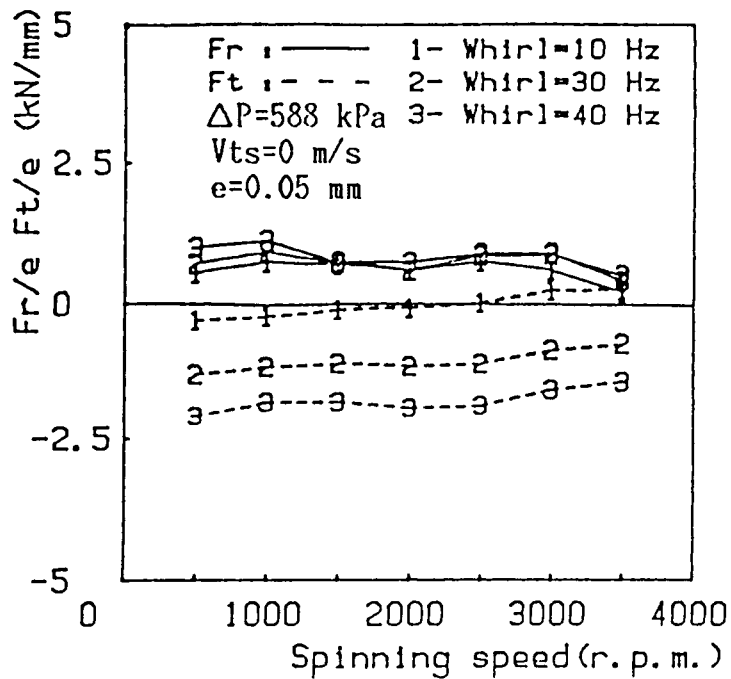
Fig.15 Force coefficients for spinning speed

6.2 Fluid force

6.2.1 Effect of spinning speed

Fig. 15 illustrates the experimental results of fluid force coefficients F_r/e and F_t/e for rotor spinning speeds. These results show that F_r/e does not

obviously vary with the spinning speed, but Ft/e increases with the spinning speed. That is, increasing the spinning speed has a destabilizing effect on the rotor system. The changes of Fr/e and Ft/e with spinning speed are independent of the pressure and the whirling amplitude, and these tendencies appear to be the same for all four types of seal.

The radial and the tangential forces (i.e., Fr/e and Ft/e) for the ratios Ω/ω are shown in Fig. 16 where the oblique fillet is the destabilizing region of Ft/e. It is known from the results that Fr/e and Ft/e vary with the spinning speed, even if the ratios of Ω/ω are the same. This may be due to fluid viscosity.

6.2.2 Effect of preswirl velocity

Fig. 17 shows the effect of the whirl ratio Ω/ω on Fr/e and Ft/e of seal 1 for various preswirl velocities. The results illustrate that the preswirl in the same direction as the spinning affects the unstable area of fluid force greatly. The preswirl in the direction of rotation extends the unstable area, but the preswirl in the direction opposite to that of rotation reduces the area, even reducing it to negative values for enough opposing swirl. However, for both of the swirls the intersection point of Ft/e and the zero axis approach about $\Omega/\omega = 0.5$ with increasing spinning speed.

This phenomenon is illustrated as the relation between the whirling speed and the average circumferential velocity rotating about $\omega R/2$. That is, when the whirling angular velocity of the rotor is lower than the average angular velocity of the fluid, the whirling motion of the rotor will be accelerated by the rotating fluid; conversely, when the whirling angular velocity is faster than the average angular velocity, the whirling motion will be restrained, so that the sign reverses about $\Omega/\omega = 0.5$. The circumferential velocity distributions in radial are shown in Fig. 18 where Figs. (b) and (c) are for the cases of enough preswirl and inverse preswirl velocities. The distribution demonstrates that the preswirl strengthens the fluid average velocity Vm, and the opposing preswirl weakens the average velocity Vm. From these effects, the unstable area varies.

In summary, the preswirl in the direction of the rotor rotation has a destabilizing effect on the rotor system, and the opposing preswirl has a stabilizing effect on the rotor system.

6.2.3 Effect of pressure difference

Fr/e and Ft/e are measured for various pressure differences between the inlet and outlet of the seal. The results show that Fr/e and Ft/e only change their values; they do not change their qualitative characteristics. One of these results is shown in Fig. 19.

6.2.4 Effect of seal length

The effect of seal length is shown in Fig. 20. The result shows that the two seals have the same tendencies for Ft/e, but not for Fr/e. Compared with that of the long seal (L/D = 1), the Fr of the short seal (L/D = 0.5) acts as a stabilizing force. This is because if the axial flow velocity increases, the tangential force which is generated by the circumferential flow decreases with the decrease of the time it takes for the flow to pass through the seal.

6.2.5 Effect of whirling amplitude

Fig. 21 shows the effect of whirling amplitude (eccentric ratio) on Fr/e and Ft/e of seal 1. The results show Fr/e and Ft/e increase with increasing whirling amplitude.
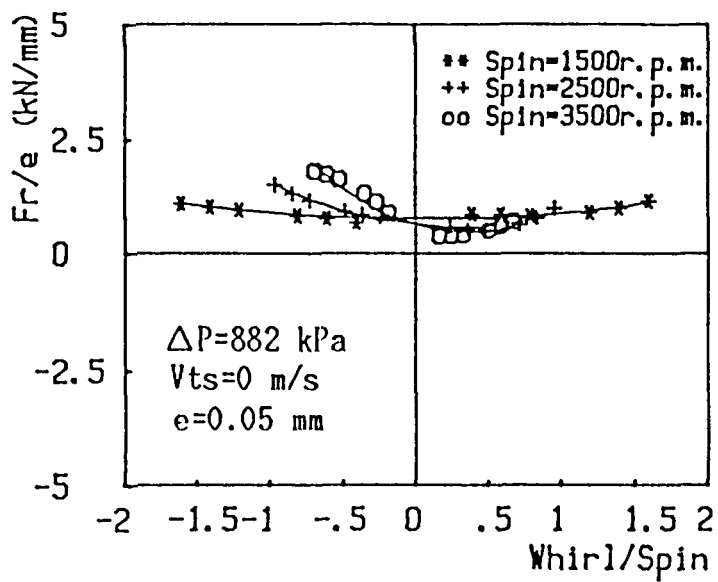
(a) Radial coefficient Fr/e
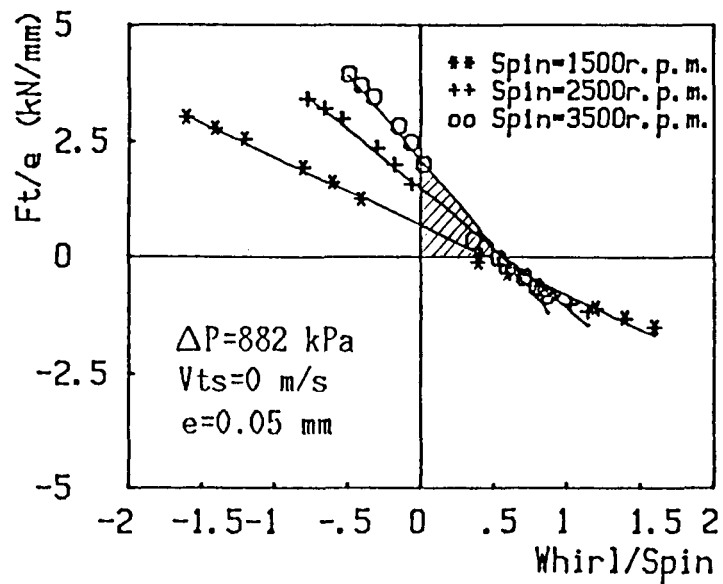
(b) Tangential coefficient Ft/e

Fig.16 Effect of spinning speed on force coefficients

243
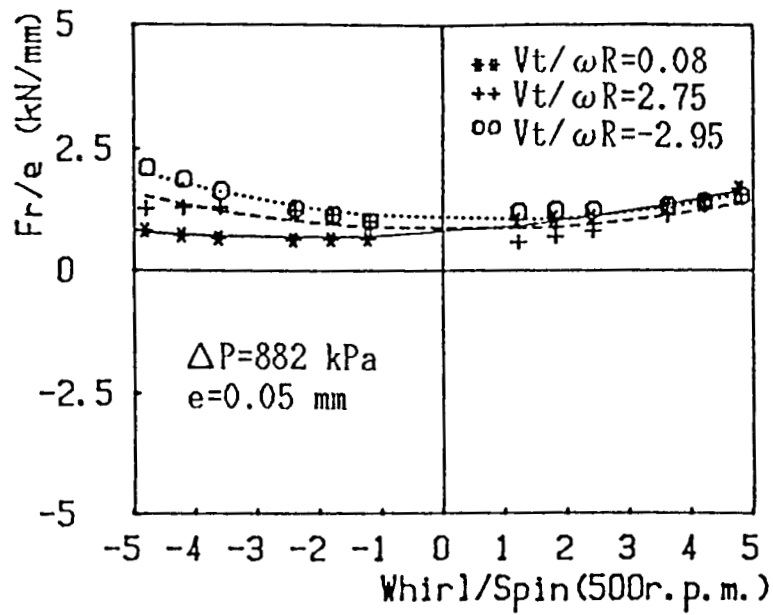
(a) Radial coefficient Fr/e
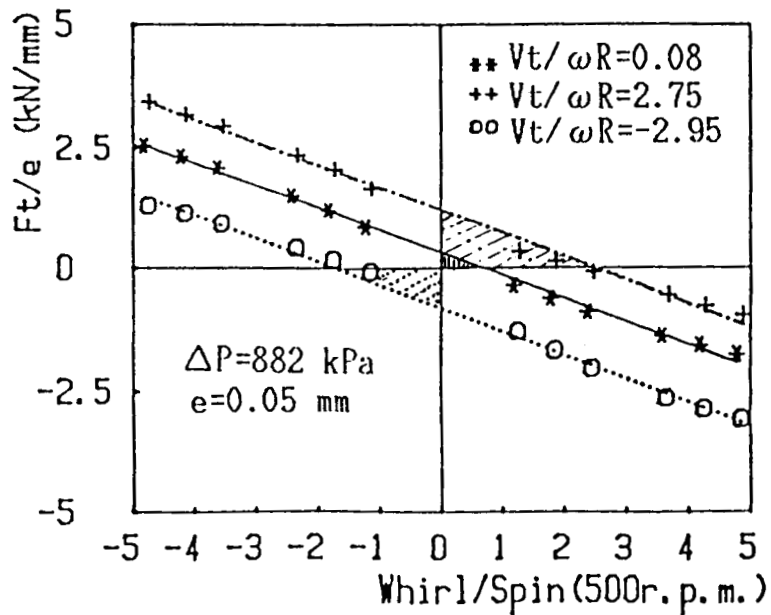
(b) Tangential coefficient Ft/e

Fig.17 Effect of swirling velocity on force coefficients

(a) Without swirl   (b) Positive swirl   (c) Negative swirl
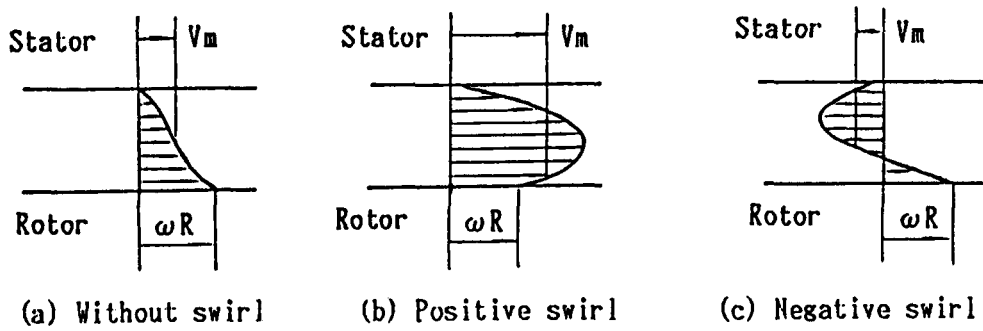
Fig.18 Velocity distributions in clearance of seal
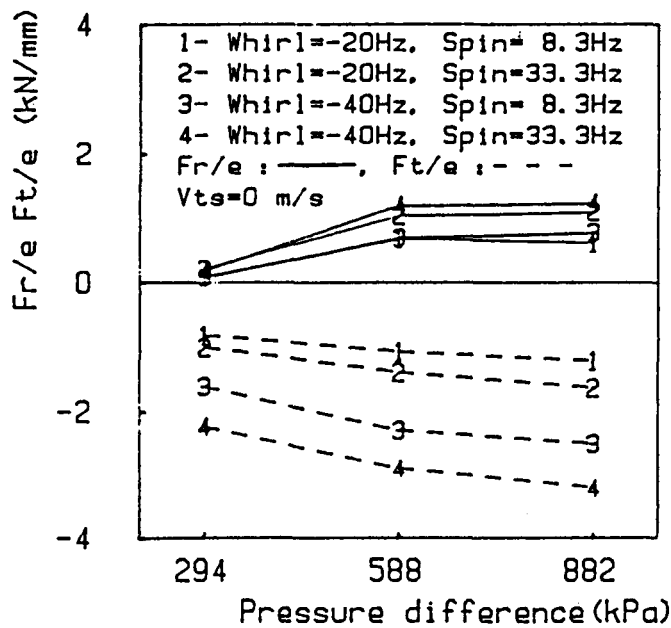
Fig.19 Effect of pressure difference on force coefficients

6.2.6 Effect of seal clearance

The results of Fr/e and Ft/e for different radial seal clearances are shown in Fig. 22. They are measured in the condition of positive preswirl velocities. Attention should be paid to Fr/e; that is, regardless of the seal length (L/D = 1.0 and L/D = 0.5), seals with large clearance have negative values of Fr/e, in contrast to seals with small clearance. It is considered that these negative Fr/e are caused by the increase of the axial flow in the large clearance seal. In addition, the tangential force coefficients Ft/e of the large clearance seals are much more influenced by preswirl velocity than those of the small clearance seal.

245
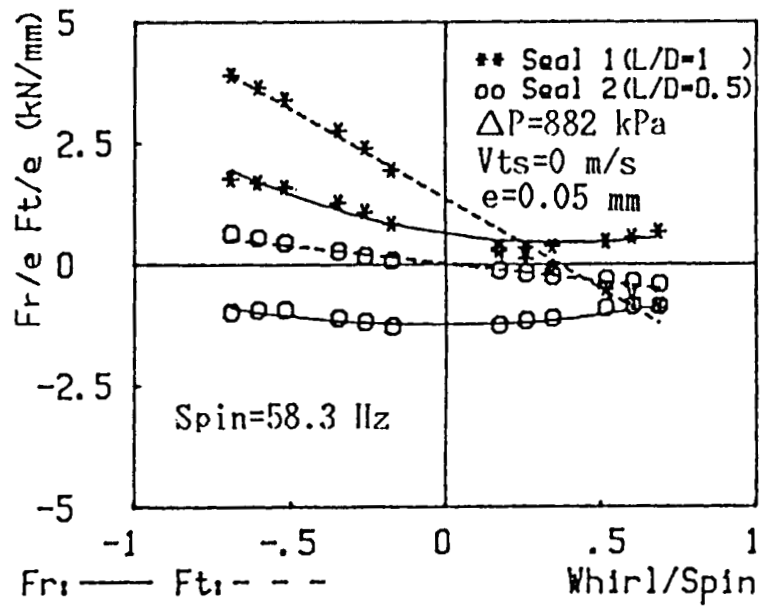
Fig.20 Effect of seal length on force coefficients
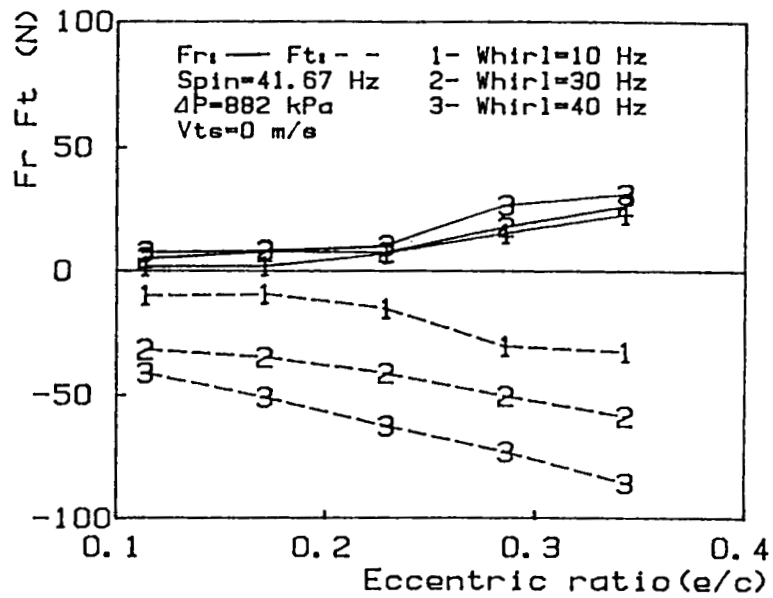
Fig.21 Forces for whirling amplitude (eccentric ratio)
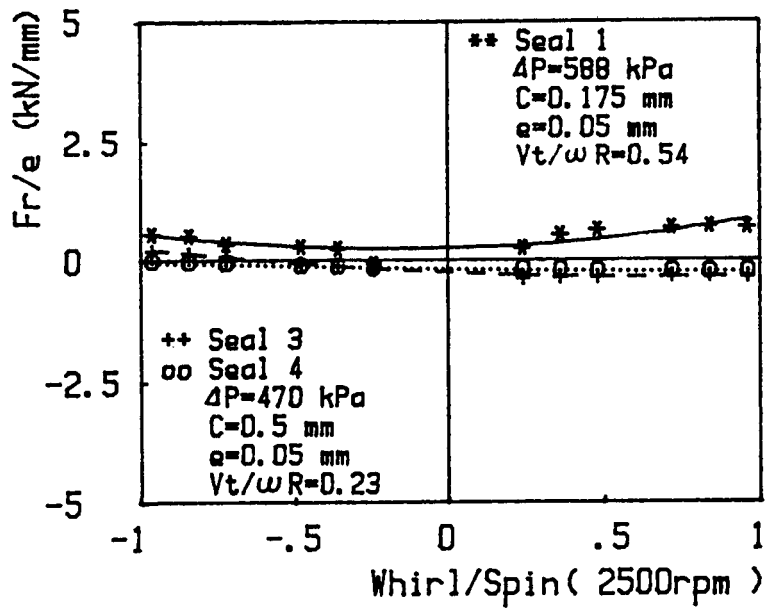
(a) Radial coefficient Fr/e
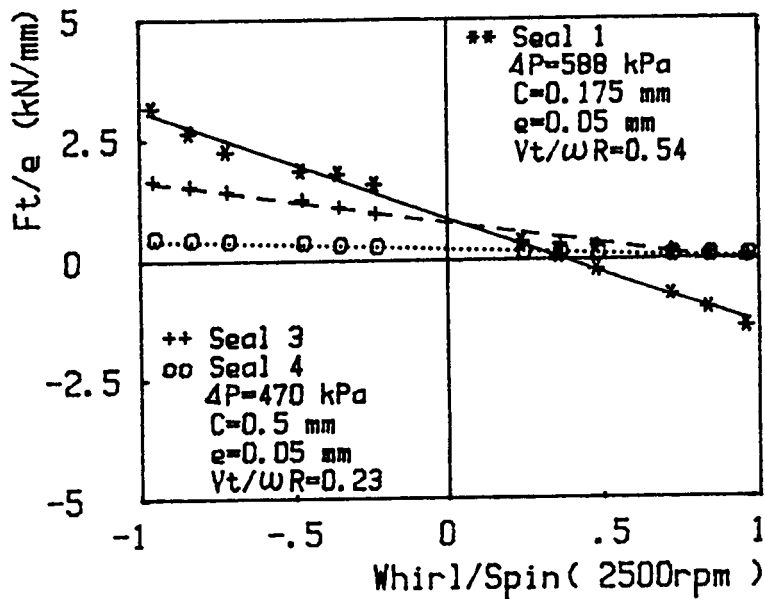
(b) Tangential coefficient Ft/e

Fig.22 Effect of seal clearance

247

6.3 Stiffness, damping, and inertia coefficients

The stiffness coefficients, damping coefficients, and inertia coefficients obtained from the fluid forces are shown in Figs. 23 and 24. These results show that the inertia coefficients are independent of the pressure difference, the eccentric ratio, and the swirl velocity, and that they always have positive values. Therefore, the inertia force decreases an eigenfrequency of the rotor system.

The direct damping coefficients are always positive and much larger than Cxy, so generally, the damping forces act as stabilizing forces on the rotor system. These damping forces are not affected by swirl velocity and seal length.

The stiffness coefficients Kxx and Kxy are largely affected by the swirl velocity, especially Kxy. These can be recognized from Fig. 23. Kxy increases with the preswirl velocity and decreases with the opposing swirl velocity. That is, the stiffness force related to Kxy may act as a stabilizing force or as a destabilizing force according to opposing preswirl or preswirl velocities.

As shown in Fig. 24, the coefficient Kxx has a negative value for the long seal 1, but Kxx has a positive value for the short seal 2. Namely, the short seal is more stable than the long seal from the view point of the stiffness coefficients of diagonal terms.

7. Conclusions

From the experimental study reported here, we derive the following conclusions:

(1) Leakage grows with increasing pressure difference, but reduces slightly with increasing spinning speed. The leakage is insensitive to the preswirl velocity, the whirling amplitude, and the whirling speed.

(2) Flow induced force increases with increasing whirling amplitude, but decreases with increasing seal clearance.

(3) Preswirl velocity strongly affects the stability of the rotor system. Preswirl velocity in the rotating direction has a tendency to destabilize, but opposing preswirl has a tendency to stabilize the rotor system.

(4) Tangential fluid force increases with rotor spinning speed; as a result, it may become a destabilizing force.

(5) Axial flow through the seal has a tendency to stablize the rotor system. It can be recognized from the radial force coefficients Fr/e of the short seal and the large clearance seal.

(6) The inertia force related to the inertia coefficient Mxx always acts to decrease the eigenfrequency of the rotor system.

(7) The damping force related to the damping coefficients Cxx and Cxy usually acts as a stabilizing force. As for the values, Cxx is larger.

(8) The preswirl velocity has no effect on Mxx, Cxx, or Cxy; however, it affects the stiffness coefficients Kxx and Kxy greatly, especially Kxy.
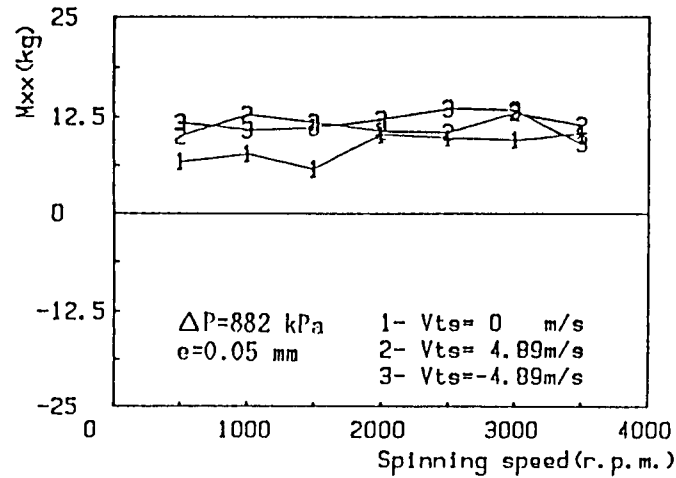
(a) Inertia coefficient
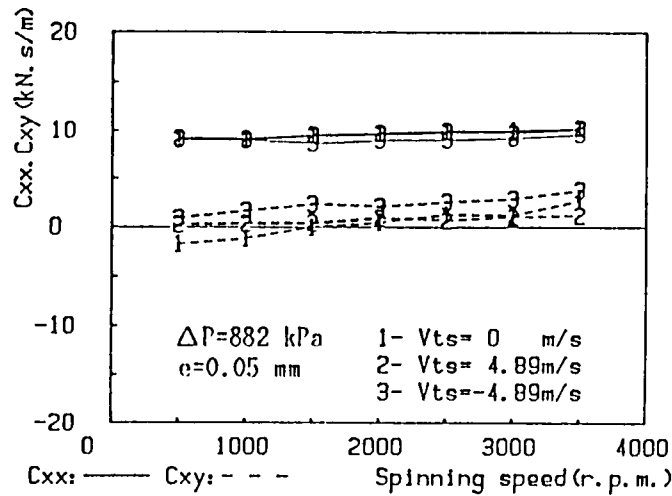
(b) Damping coefficient
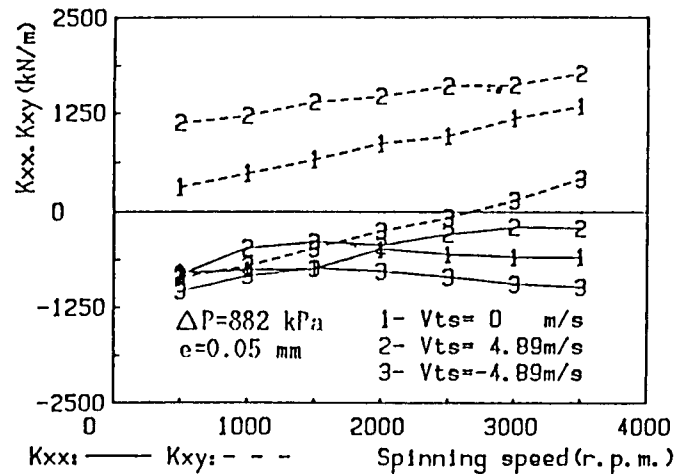
(c) Stiffness coefficient

Fig.23. Effect of swirling velocity on characteristic coefficients

249
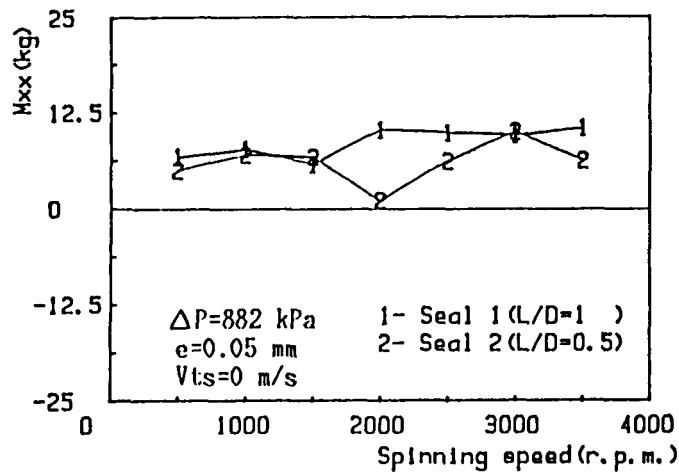
(a) Inertia coefficient
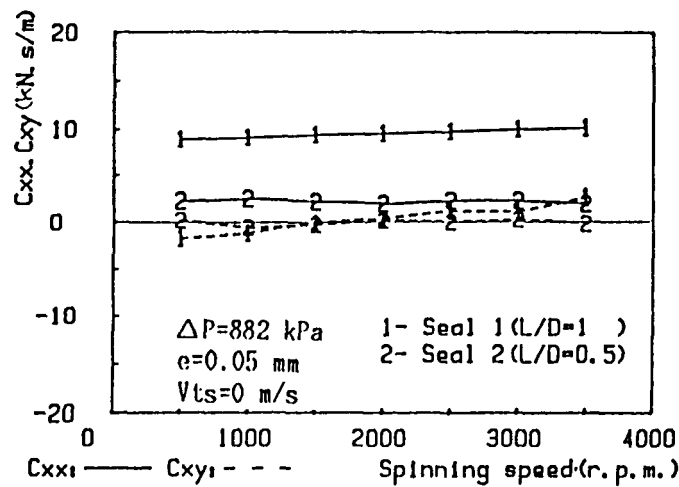
(b) Damping coefficient
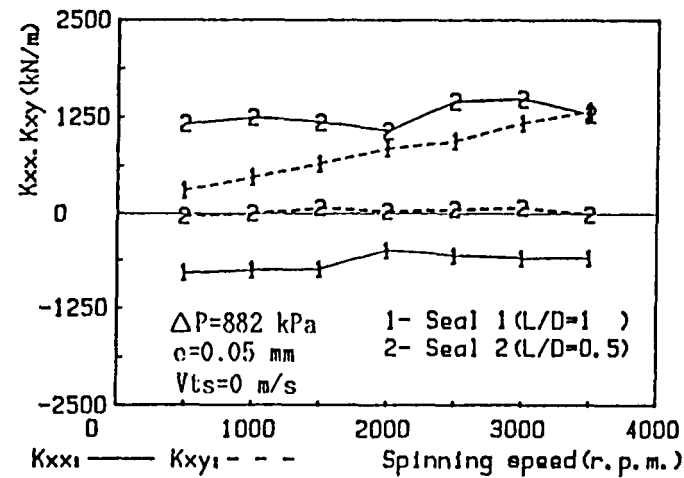
(c) Stiffness coefficient

Fig.24. Effect of seal length on characteristic coefficients

250

References

1. Black, H.F., Calculation of Forced Whirling and Stability of Centrifugal Pump Rotor System. Trans. ASME J. Eng. Ind. (1974) 1076.

2. Childs, D.W., and Kim, C.H., Analysis and Testing for Rotordynamic Coefficient of Turbulent Annular Seal With Different, Directionally Homogeneous Surface-Roughness Treatment for Rotor and Stator Elements. NASA Conf. Pub. (1982) 313.

3. Childs, D.W., Dynamic Analysis of Turbulent Annular Seal Based on Hirs' Lubrication Equation. Trans. ASME No. 82-Lub-41.

4. Nordmann, R., and Massmann, H., Identification of Stiffness, Damping and Mass Coefficients for Annular Seals. I. Mech. E. (1984) 167.

5. Iwatsubo, T., Evaluation of Instability Forces of Labyrinth Seal in Turbine or Compressors. NASA. Conf. Pub. (1980) 139.

6. Yang, B.C., Iwatsubo, T., and Kawai, R., A study on the Dynamic Characteristics of Pump Seal. (1st Report, In Case of Annular Seal with Eccentricity) Trans. JSME, Vol. 49, No. 445. (1983) 1636.

7. Kaneko, H., Iino, T., and Takagi, M., An Experimental Research on Dynamic Characteristics of Annular Pump Seals. (1st Report, Dynamic Characteristics in Case of Concentricity) Proc. JSME, No. 820-3 (1982) 25.

8. Kanki, H., and Kawakami, T., Experimental Study on the Dynamic Characteristics of Pump Annular Seals. I. Mech. E. (1984) 159.

9. Kaneko, S., Hori, Y., and Tanaka, M., Static and Dynamic Characteristics of Annular Plain Seals, I. Mech. E. (1984) 205.

10. Kanemori, Y., and Iwatsubo, T., Experimental Study of Dynamic Characteristics of Long Annular Seal. Proc. 2nd China-Japan Joint Conf., Xi-an (1987) 143.